Selective-adsorption line shapes in the scattering of ^{4}He by LiF(001)

David A. Wesner and Daniel R. Frankl
Department of Physics, The Pennsylvania State University, University Park, Pennsylvania 16802
(Received 2 April 1981)

Selective-adsorption line shapes were experimentally studied in 17-meV ^{4}He-atom scattering from a LiF(001) crystalline surface. The specular and several diffracted beams were measured for a variety of incidence conditions. Specular line shapes obey the three rules put forth by Wolfe and Weare. The specular and diffracted-beam line shapes obey the rules formulated recently by Celli, Garcia, and Hutchison in all cases except for the specular Wolfe-Weare rule-2 case. In this case the mixed-extrema structure predicted by Wolfe and Weare is seen. This line shape is very sensitive to surface temperature and age, confirming a recent prediction of Wolfe and Weare concerning inelastic effects on the selective-adsorption line shapes.

I. INTRODUCTION

Since the work of Stern *et al.*[1] and Lennard-Jones and Devonshire[2] in the 1930's, the phenomenon of selective adsorption has been recognized as a useful tool for elucidating details of the gas-atom – surface interaction. Studies have yielded information on the surface potential well,[3] the corrugation of the repulsive potential parallel to the surface,[4] and more recently, inelastic scattering effects.[5,6] However, successful theoretical predictions of selective-adsorption line shapes are relatively recent. In this article we report an experimental test of recent theoretical predictions by Celli, Garcia, and Hutchison[7] and by Wolfe and Weare.[8,9] The experiments include measurements of selective adsorption features in several diffracted beams for a variety of incidence conditions of ^{4}He-LiF. This part is similar to an earlier investigation by Liva and Frankl[10] for the ^{4}He-NaF system. In addition we made measurements on the effects of inelasticity and surface cleanliness on the selective-adsorption line shapes.

II. SELECTIVE-ADSORPTION LINE SHAPES

Selective adsorption dominates much of the detailed structure seen in the scattering of low-energy gas atoms from crystalline surfaces. It is a resonance between the incoming-free-particle state and a state in which the particle is bound in the attractive potential well perpendicular to the surface while simultaneously translating as a nearly-free particle parallel to the surface. A transition into such a bound state conserves the parallel part of the wave vector modulo a surface reciprocal-lattice vector. The requirement of energy conservation then yields the approximate kinematic equation for elastic selective adsorption,

$$(\vec{K} + \vec{G}_{m,n})^2 = |\vec{k}_i|^2 + \frac{2M}{\hbar^2}|E_j| \tag{1}$$

where $\vec{k}$ is the incident wave vector, $\vec{K}$ its projection on the surface, M the atom mass, and E_j is the jth (negative) energy eigenstate of the atom-surface potential well. The surface reciprocal-lattice vector $\vec{G}_{m,n}$ is given by

$$\vec{G}_{m,n} = m\hat{g}_1 + n\hat{g}_2 \tag{2}$$

with m,n integers and $\hat{g}_1,\hat{g}_2$ the surface reciprocal-lattice basis vectors. We denote the resonance defined by Eq. (1) as a $j(m,n)$ selective adsorption. Equation (1) ignores any Bloch wave character in the selectively adsorbed state, an approximation which is good in regions of $\vec{K}$ space remote from degeneracies [i.e., two or more sets of $j(m,n)$ which simultaneously satisfy Eq. (1)]. Because the atom-surface potential well has discrete energy eigenstates, a selective adsorption may occur only for certain incident wave vectors, the loci of which are given by Eq. (1) (see Fig. 1). Thus if the experiment monitors a diffracted beam intensity as a function of, for example, θ, the polar angle of $\vec{k}$ with respect to the surface normal, some sort of feature should be seen when then be used to determine the E_j. For ^{4}He-LiF this has been done, and the eigenvalues are known to fairly high accuracy for $j = 0$, 1, 2, and 3.[11]

A theoretical prediction of the exact line shape of a given selective adsorption feature can, of course, come only from consideration of the dynamics of

the scattering. Early elastic theories predicted that the features seen in the specular intensity, I_{00} versus incident angle, should be maxima. This was consistent with the notion that the onset of a selective adsorption opened an additional channel whereby the atom might rejoin the outgoing specular beam. In the early experiments, however, mostly minima were observed. It was assumed that inelastic processes operating while the atom was selectively adsorbed removed it from the elastic scattering process.

Chow and Thompson[12] developed the first elastic theory that yielded minima as well as maxima for the selective adsorption features. Their method involved numerical solution of the coupled differential scattering equations for a corrugated-hard-wall potential. A later version [13] used a more realistic potential and obtained similar results. The calculations also showed that certain diffracted beams could show maxima under conditions coincident with a specular-beam minimum, a result expected on unitarity considerations alone. These results agreed qualitatively with the measurements of Wood, Mason, and Williams[14] and Liva and Frankl.[10]

More recently there has been interest in the derivation of more general rules which predict selective-adsorption line shapes. Wolfe and Weare[8] have proposed three rules which correlate the specular-beam line shapes with Fourier components of the potential and with other diffracted channels. For an isolated (nondegenerate) selective adsorption, the rules may be summarized as follows: (1) A minimum will be observed when the resonance couples strongly to the specular beam and to at least one other open diffraction channel. (2) A "mixed-extrema" structure (a maximum on one side and a minimum on the other side of the resonance point) occurs if the only open channel to which the resonance couples strongly is the specular. The predominant feature, however, is the maximum, which is closer to the resonance point. (3) A maximum results if the resonance does not couple strongly to the specular channel. In practice, for ^{4}He-LiF, strong coupling means that the two $\vec{G}$'s in question, one pertaining to the resonance and one to an outgoing beam, are separated by a first-order reciprocal-lattice vector, i.e., either (0,1) or (1,0). Ultimately this is related to the relative strengths of successive Fourier components of the atom-surface potential:

$$V(\vec{r}) = V_0(z) + \sum_{\vec{G}\neq 0} V_{\vec{G}}(z) e^{i\vec{G}\cdot\vec{R}} \quad . \tag{3}$$

Here $\vec{r}$ is composed of $\vec{R}$ parallel to the surface, z perpendicular to it, and V_0 represents the lateral average of V and contains the attractive well. The Fourier terms $V_{\vec{G}}(z)$ give the corrugation of the repulsive part of the potential. Goodman has shown[15] that the early theory of Cabrera *et al.*,[16] formerly thought to yield only specular maxima, can also yield the three types of behavior predicted by Wolfe and Weare and a similar set of rules. The predictions of the Wolfe-Weare rules agree very well with the ^{4} He-LiF data of Frankl *et al.*[17] Agreement with ^{4}He-graphite data is not as good.[5] This is believed to be due to inelastic effects in that system (see below).

Both the work of Goodman and that of Wolfe and Weare pertain to specular-beam line shapes. The work of Celli, Garcia, and Hutchison[7] encompasses both specular and diffracted beams. Their results were derived for a corrugated hard wall with an attractive potential well. This approximation involves assuming $V_0(z)$ in Eq. (3) infinite for $z \leq z_0$, the corrugation parallel to the surface coming from a periodic variation of z_0 with $\vec{R}$. If the corrugation has a simple sinusoidal variation with rectangular symmetry, then an isolated selective-adsorption line shape for any diffracted beam can be shown to have an intensity

$$I(x) \propto 1 + \frac{b(b+2)}{1+x^2} \quad . \tag{4}$$

Here b is a real parameter whose sign is determined by $(-1)^l$, with l given by

$$l = \tfrac{1}{2}(\,|m| + |m'-m| - |m'| + |n| + |n'-n| - |n'|\,) \quad , \tag{5}$$

where (m,n) represents the resonance state and (m',n') the diffraction beam in which the resonance is observed. The quantity x in Eq. (4) is related to how far away the incident conditions are from a resonance point, $x = 0$ being the point at which Eq. (1) is satisfied. Equation (4) is valid for $|x| < 1$, i.e., near the resonance. These equations predict a Lorentzian line shape which is a maximum for $b > 0$ (l even), and a minimum for $0 > b > -2$ (l odd). Equation (5) thus constitutes a useful rule for determining the line shape in any particular beam. For $b < -2$ a maximum again obtains, which the authors interpret as arising from a selective adsorption in a region where the background intensity is small and the selective adsorption overwhelms it. This is because the magnitude of the parameter b measures the ratio of resonant intensity to background intensity. Note that Eq. (4) predicts no

mixed-extrema line shapes like those of rule 2 of Wolfe and Weare.

This theory was found to agree well with existing data. It also agrees well, within its region of applicability, with a calculation by Chow[18] of I vs θ curves for ^{4}He-LiF for several diffracted beams. Chow's method was an iterative Green's-function solution of the coupled scattering equations using a Morse potential.

Of course, inelastic effects are still believed capable of producing selective-adsorption minima. This was seen experimentally for ^{4}He-graphite by Wesner *et al.*[5] and Boato *et al.*[19] when the Wolfe-Weare predictions were found to be violated for certain resonances. Theoretically predicted maxima were observed as minima. Chow[20] has used an optical potential to treat inelastic effects phenomenologically in an otherwise elastic scattering model. The results show that resonance maxima turn more or less uniformly into minima as the strength of the imaginary part of the potential is increased. There is also an overall blurring effect on the structure. Hutchison[21] has found similar effects by modifying the scattering amplitudes arising in the work of Celli *et al.*[7] by the inclusion of a Debye-Waller prefactor. Wolfe and Weare[9] have used an optical potential in an extension of the method of Harvie and Weare,[22] and find that a small imaginary part in the potential (of magnitude 0.1 meV) is sufficient to turn a rule-2 maximum into a minimum. They also note that the rule-2 maxima in particular seem unusually sensitive to this effect. For example, the 0.1 meV imaginary term in the potential did not appreciably affect the width or shape of other (rule 1 or 3) resonances. These only began to show effects at larger values of the imaginary potential parameter.

III. EXPERIMENTS

A. Apparatus

The apparatus used is substantially the same as that used in our previous investigations.[5,23] We will describe in detail only new features or those important to the present work. The ^{4}He beam is produced by a supersonic nozzle at 77 K, which results in a nearly monochromatic ($\Delta v/v < 2\%$) low-energy (~ 17 meV, $k_i = 5.76$ Å^{-1}) beam. It is well collimated ($\Delta\theta < 10^{-3}$ rad) before entering the scattering chamber in a horizontal direction. At the surface the beam is about 1 mm in diameter. The sample surface, LiF(001), has two rotational degrees of freedom: the polar angle rotation θ about a vertical axis tangent to the surface, and the azimuthal rotation ϕ about a horizontal axis perpendicular to the surface. The detector is a quadrupole mass spectrometer mounted on an arm that rotates about a vertical axis collinear with the sample rotation axis. The detector sensitive region is located about 56 mm from the surface. The detector can scan the specular intensity as a function of θ and it is possible to vary its height above the plane of incidence and thereby measure out-of-plane diffracted beams as well. The detector aperture is a vertical slit, approximately 5 mm tall by 1 mm wide, the height allowing out-of-plane diffracted beams to enter the active detector volume at an angle.

Two different detector geometries were used for this study. They differ only in the geometry in which the incident gas atoms are ionized, the subsequent extraction, filtering, and multiplication stages being identical. Both detectors ionize the atoms by electron impact and use various lenses to draw them into the quadrupole filter. In one configuration, hereafter referred to as detector I, the beam enters the ionization region antiparallel to a ribbon-shaped stream of electrons of mean energy about 100 eV. Detector II has a similar electron stream, but the atoms enter at a 90° angle to it. Detector I allows some electrons to escape the detection region through the incoming beam aperture slit and probably reach the sample surface. Detector II is more enclosed and any stray electrons that do escape are aimed away from the surface. The advantage of detector I is that it has a very narrow angular sensitivity characteristic, desired in a different application but not essential to the work described here.

Two methods of sample preparation were used: heat treatment in vacuum or *in situ* cleavage. The former involves first a chamber bakeout to an ultimate pressure of about 8×10^{-8} Pa. Then the sample is heated to about 850 K for 50–60 h, the background pressure rising to about 7×10^{-7} Pa. After the sample is cooled, the pressure comes back to about 1×10^{-7} Pa. Unless otherwise noted, all of our data were taken with the surface cooled to about 150 K. Between data runs, when the surface returns to room temperature the background pressure is about 4×10^{-7} Pa. The second method involves cleaving a small piece from the front of a bar-shaped crystal, exposing a clean surface. The bar can be successively advanced in the holder so that a dozen or more cleaves are possible without breaking the vacuum. In this method the only sample heating is to about 400 K (to outgas the holder), concurrent with the chamber bake. Correspondingly, the background pressure is about 9×10^{-8} Pa (5×10^{-8} Pa with the surface cooled). The two

methods employ different sampler-holder arrangements, since the heat treatment requires a low thermal mass. Thus for the heat treatment a much smaller piece of crystal is used. It may, however, be cleaved *in situ* once, prior to the heat treatment.

Samples prepared in either of these two ways show degradation with time, even at a continuous background pressure in the 10^{-8}-Pa range. Typically this degradation is rather slow, allowing the surface to be used for more than a week before either a fresh cleave or reheating of the sample is necessary. Generally the degradation takes the form of a decrease in the reflected beam intensities, the selective-adsorption line shapes and other features of the scattering pattern simply scaling down. However. an exception is discussed below.

B. Results

We measured the intensity of the specular beam and several diffracted beams as functions of polar incidence angle θ in four different regions of $\vec{K}$ space. These were chosen to provide a wide variety of selective-adsorption conditions: resonances of all three Wolfe-Weare types, isolated and degenerate resonances, resonances at oblique and near-glancing incidence, and resonances along symmetry and nonsymmetry azimuthal directions. Figure 1 is a $\vec{K}$-space diagram illustrating the four regions scanned. The circle arcs are the loci of points satisfying Eq. (1). Typically a specular or diffracted beam was scanned through a range of θ with ϕ held fixed. In the $\vec{K}$-space diagram this corresponds to movement along a portion of a ray through the origin ($\theta = 0°$), making an angle ϕ with the K_x direction. Many of the data were taken at least twice, once with detector I and a heat-treated surface, and once with detector II and a cleaved surface. The latter combination proved better in the sense that larger reflection intensities were observed and more detailed structure could be seen in the scans. However, for the most part the results with detector II and a cleaved surface confirmed those of detector I and a heat-treated surface.

At this point it should be mentioned that in all the figures that follow, the sample polar angles given are only nominal values and may be in error by about $\pm 1°$. Because accurate measurements of E_j were not our goal, we did not carry out any of the procedures[24] for zeroing the polar angle. There may also be variations in the location of certain features from one scan to another, also typically one degree or less. They are related to the difficulty of returning the beam laterally to exactly the same location on the surface after it has been moved away to measure the incident intensity. Variation between the two holders used for cleaved and heated samples caused a similar error. We did, however, zero the azimuthal rotation angle by study of the symmetry of the scattering patterns.

Figure 2 contains diagrams for each of the four

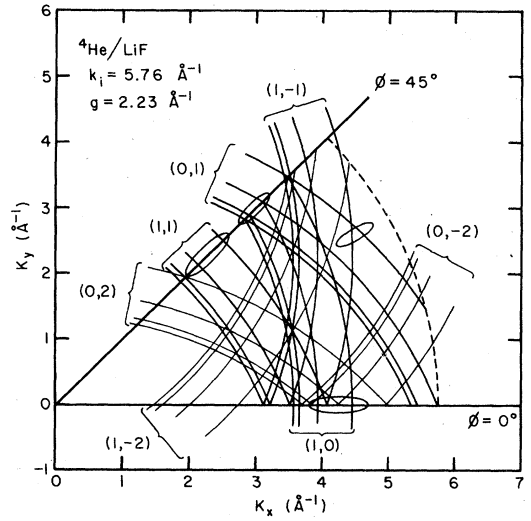

FIG. 1. $\vec{K}$-space diagram showing the loci of incidence conditions satisfying Eq. (1). The $\vec{G}$'s of the resonances are labeled. The four ellipses enclose the approximate regions of $\vec{K}$ space represented by the data of Figs. 3 through 9.

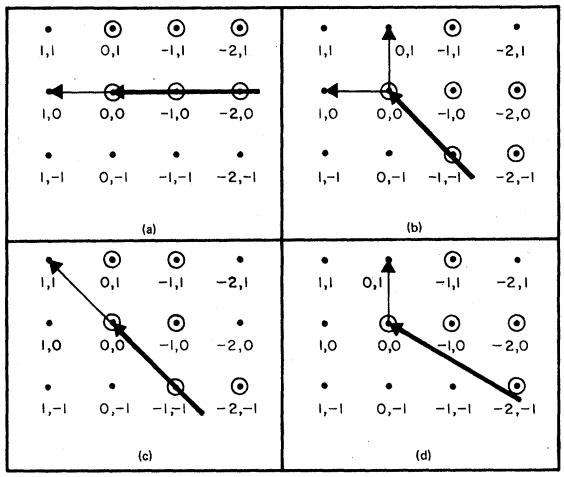

FIG. 2. Reciprocal-space diagrams for the four regions of $\vec{K}$ space scanned; (a) through (d) correspond to Figs. 3 through 6, respectively. The incident parallel wave vector is a heavy arrow, the resonance $\vec{G}$ a lighter arrow, and the diffraction beams that were measured are circled.

regions of $\vec{K}$ space, illustrating the relationships among the resonance, the incident state, and the various diffracted beams. Figures 3 through 6 display our results for specular and diffracted-beam intensities in the four regions of $\vec{K}$ space. All of the data presented are for detector II and a cleaved surface, but nearly all were confirmed by measurements with detector I and a heated surface. Several above-plane and in-plane diffracted beams, in addition to the specular, were monitored in each region.

Figure 3 shows results for $\phi = 0°$, $\theta = 43° - 53°$. A 0(1,0) selective adsorption is expected near $\theta = 51°$. The transition to the next level, 1(1,0), should be near $\theta = 44°$ but from about 48° down, this region of $\vec{K}$ space is relatively crowded, as can be seen from Fig. 1. Second- and third-order resonances are possible, and it is hard to distinguish the 1(1,0). Figure 4 shows the polar-angle range $43° - 53°$ at the $\phi = 45°$ azimuth. Here the 1(1,0) and 2(1,0) resonances near $\theta = 48.5°$ and 44.5°, respectively, are degenerate with the corresponding (0,1) levels. The same azimuth, $\phi = 45°$, but a more oblique polar-angle range is shown in Fig. 5. Isolated 0(1,1) and 1(1,1) resonances are expected near $\theta = 37°$ and 30°, respectively. A higher-order resonance, the $0(-1,2)$ degenerate with $0(2,-1)$ is possible near $\theta = 33°$. Finally, a nonsymmetry azimuth, $\phi = 30°$, is shown in Fig. 6 for the more glancing polar-angle range of $\theta = 60° - 70°$. A 0(0,1) resonance near $\theta = 66°$ and a $0(1,-1)$ near $\theta = 63°$ are expected. With the exception of the lower θ range of Fig. 3, all of these regions of $\vec{K}$ space are relatively "clean," i.e., there are no in-

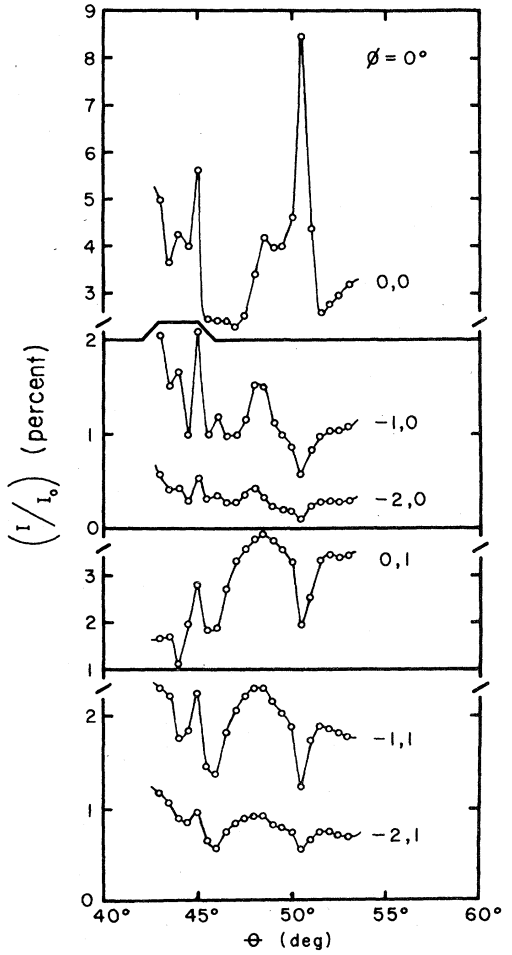

FIG. 3. Diffraction beam intensities at $\phi = 0°$, $\theta = 43°$ to 53°. Note that all of the intensities are normalized to the incident intensity, I_0, but that different beams generally have different ordinates. The detector-II—cleaved-surface combination was used.

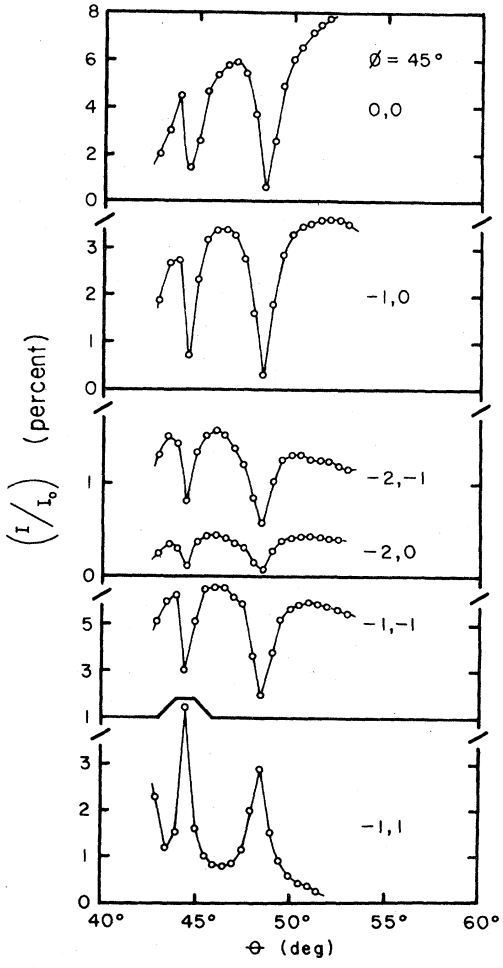

FIG. 4. Similar to Fig. 3, but for the region $\phi = 45°$, $\theta = 43°$ to 53°.

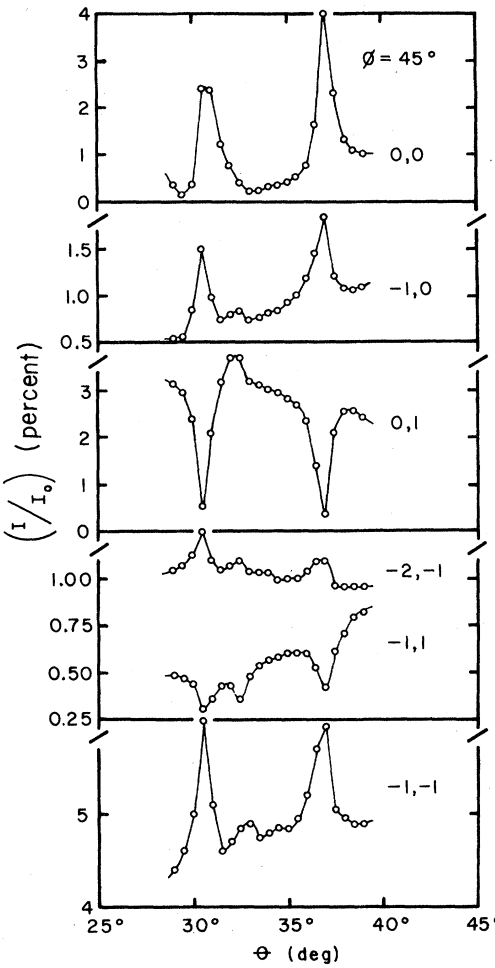

FIG. 5. Similar to Fig. 3, but for the region $\phi = 45°$, $\theta = 29°$ to $39°$.

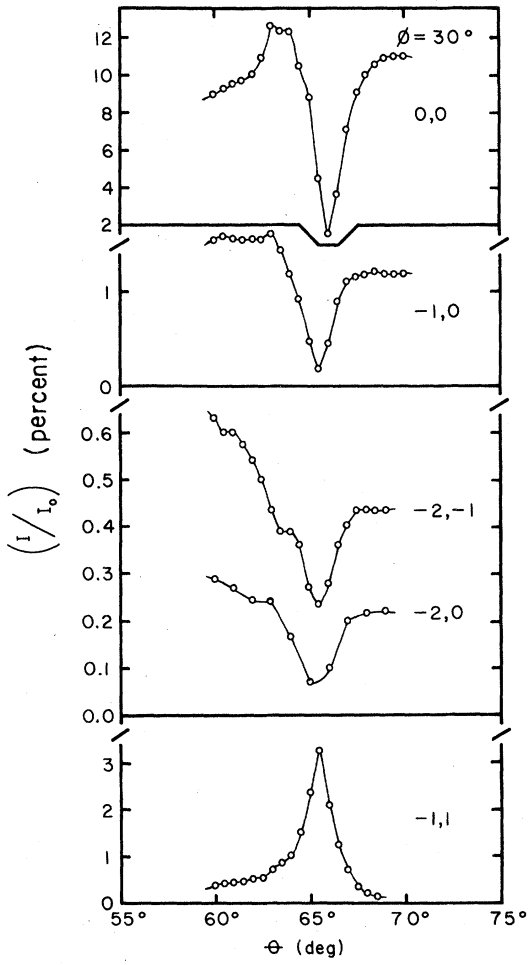

FIG. 6. Similar to Fig. 3, but for the region $\phi = 30°$, $\theta = 60°$ to $70°$.

terfering higher-order resonances near the ones of interest. The data of Figs. 3 through 6 were taken within six days of cleaving.

The behavior of the specular intensity at the 0(1,0) resonance near $\theta = 51°$, $\phi = 0°$, in Fig. 3 was quite unique. It was the only feature in any of the beams studied whose line shape was markedly different with the detector-I—heated-surface combination than with detector-II—cleaved surface. In the former it was a minimum, in the latter a maximum. Several more experiments were done with the specular beam of Fig. 3 to investigate this.

Figure 7 shows this beam's dependence on sample temperature; Fig. 8 displays the effect of surface age. Both of these were measured with detector II and a cleaved surface. The scans at four different sample temperatures in Fig. 7 were taken within a few hours of each other about four days after the sample had been cleaved. The three scans in Fig. 8 show the effects of time elapsed since cleaving, ranging from less than an hour to six days. In the interim between these scans the sample was maintained at a pressure of 9×10^{-8} Pa or lower. There were also several thermal cycles between room temperature and 150 K, while other data were being taken.

One final experiment was done with the specular beam and the incidence conditions of Fig. 3. Detector II was used to study the reflection from a heat-treated surface. This surface received a bake at 850 K, as did those studied with detector I, but only for about 20 h instead of 50—60 h. Figure 9 shows the results, the data being taken a few hours after cooling the crystal. The scan was inadvertently taken at $\phi = 2.6°$ instead of 0°, but the neighborhood in $\vec{K}$ space is virtually the same. The 0(1,0) feature is now near $\theta = 52°$. Another difference between this scan and those reported above is that the sample temperature was about 100 K rather than 150 K as

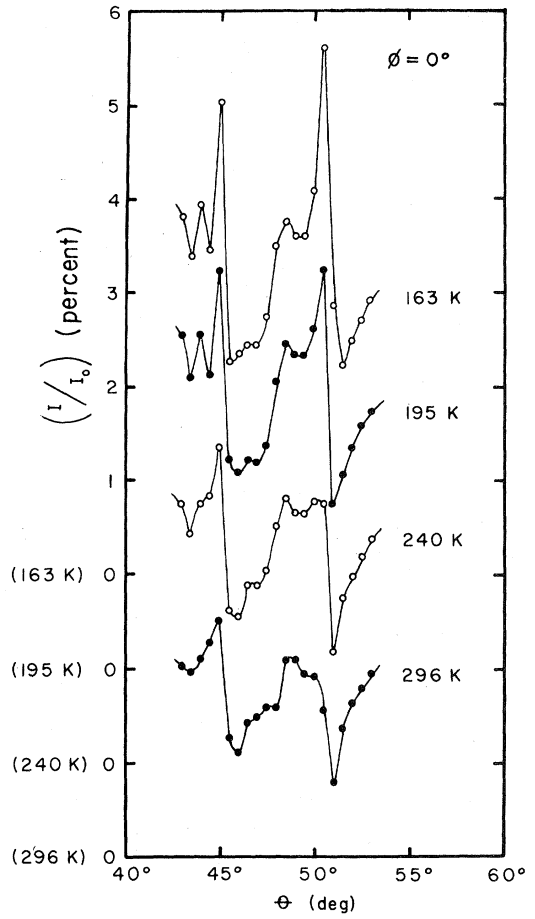

FIG. 7. Temperature dependence of the specular-beam intensity for the same incidence conditions as in Fig. 3. The sample temperature is indicated next to each scan. Ordinates of successive scans are shifted downward for clarity.

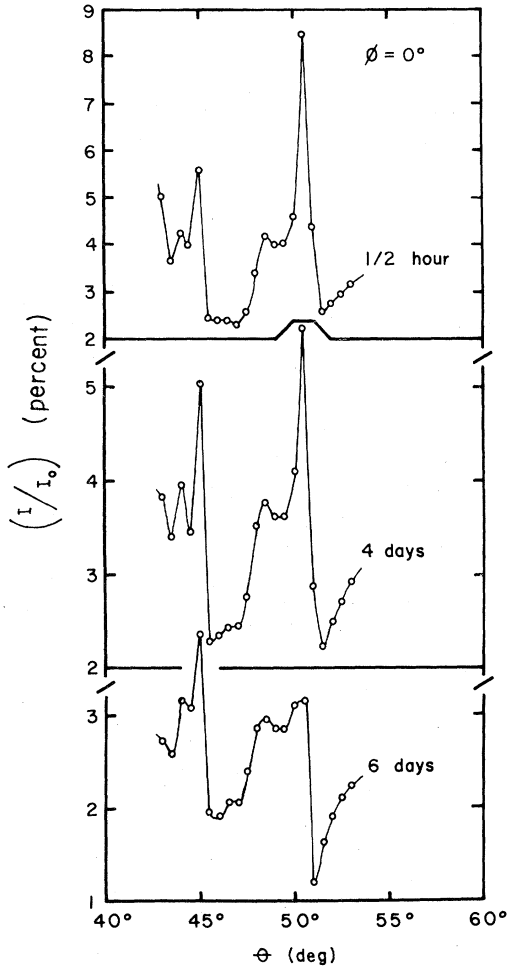

FIG. 8. Aging effect on the specular-beam intensity, incidence conditions as in Fig. 3. Time elapsed since cleaving is indicated next to each trace.

a result of an improvement in the liquid-nitrogen sample-cooling arrangement. A relatively rapid deterioration with time was observed with this sample, reflected by a significant loss of specular intensity within a day of ending the sample bake.

A word should be said about the fourth possible permutation of detector geometry and surface preparation method: detector I and a cleaved surface. Several attempts were made to take data with this combination, with varying degrees of failure. The results were highly variable and difficult to quantify, but in general much more rapid rates of deterioration of the surface reflection intensity were observed than with the other detector-sample combinations. This deterioration was evidently connected with bombardment by the ionizing electron stream in detector I. In some cases decay of specular reflection intensity was seen to occur in the short time it took to turn up the ionizer emission current to its full value (several seconds). Afterward the ultimate amount of specular reflection was less than 1% under conditions where the other detector-sample combinations gave about 10%. Other times the reflected signal was more stable and intense, but never as good as seen with the other combinations. Several times the detector-I—cleaved-surface combination was tested using the sample holder which permits one *in situ* cleave, and then subsequent heating. After measurements on the cleaved surfaces were made and deterioration was observed, the same surfaces received the heat treatment described above. They then recovered and gave the typical results described for heat-treated surfaces with detector I.

IV. DISCUSSION

Table I is a summary of the major observed selective-adsorption line shapes based on the scans

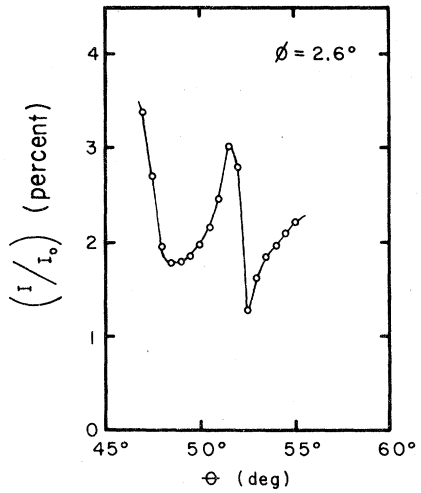

FIG. 9. Specular-beam intensity under approximately same incidence conditions as in Fig. 3, but measured with the detector-II—heated-surface combination.

in Figs. 3 through 6, compared with the predictions of Celli *et al.*[7] and Wolfe and Weare.[8] The former are based on Eq. (5), the latter on the three rules outlined in Sec. II. Note also that the predictions have been applied to some selective adsorptions for which they are ostensibly not valid, i.e., the degenerate resonances shown in Fig. 4.

The specular 0(1,0) resonance near $\theta = 51°$ in Fig. 3 falls under Wolfe and Weare's rule 2 and should be a mixed-extrema structure. The scan confirms this, showing a pronounced maximum near 50.5° and a shallower minimum at 51.5°. A minimum is predicted for this resonance by the rule of Celli *et al.* This resonance was the only pronounced feature in conflict with the Celli rule. In fact, this type of feature corresponds to the exceptional case of $b \simeq -2$ in Eq. (4), the line shape then predicted by Eq. (4) being unobservable.[7,25] Celli *et al.*[7] have considered an alternative formulation based on distorted-wave-perturbation theory and similar to the approach of Wolfe and Weare. In this method Eq. (4) no longer applies, b becomes complex, and the specular intensity displays an asymmetric maximum more in agreement with Wolfe and Weare. A 0(1,0) minimum is predicted for all the nonspecular beams in Fig. 3, and is evident near 50.5° in each scan. The region $\theta < 48°$ is, as discussed above, relatively crowded and the 1(1,0) in Fig. 3 is apparently lost in the background, both for specular and nonspecular beams. However, see the discussion of Fig. 7 below.

Neither the Wolfe-Weare nor the Celli rules are strictly applicable to the data in Fig. 4 because the (0,1) and (1,0) resonances are degenerate. The data themselves show very pronounced minima for all beams except the $(-1,1)$, which is a sharp maximum. This is analogous to the behavior observed with ^{4}He-NaF by Liva and Frankl.[10] In that case a nearby beam, separated from the resonance by a first-order reciprocal-lattice vector, showed a maximum while the specular showed a minimum. Applying Wolfe and Weare's rules to the (0,1) or (1,0) resonances yields minima for both in the specular beam. Equation (5) predicts all minima for the measured diffractions in Fig. 3 if a (1,0) resonance is assumed. It predicts all minima except for a $(-1,1)$ beam maximum if a (1,0) resonance is assumed. Because of the symmetry, of course, the $(1,-1)$ beam which was not measured, should show a maximum. For this beam Eq. (5) predicts a maximum if a (1,0) resonance is used, and a minimum for a (0,1) resonance. Thus in this case the below-plane beams coupled to a (1,0) resonance are analogous to the above-plane ones coupled to a (0,1) resonance. For the majority of diffracted beams Eq. (5) predicts the same result for either resonance and is confirmed experimentally.

Figure 5 shows the isolated 0(1,1) and 1(1,1) resonances, for which both the Wolfe-Weare and Celli *et al.* predictions are confirmed. The specular and three other beams show maxima while the (0,1) and $(-1,1)$ show minima. Near $\theta = 33°$ in several of the beams is a feature which is probably the $0(-1,2)$ resonance degenerate with a $0(2,-1)$. (These higher-order resonances were omitted from Fig. 1 for clarity.) This feature is a Wolfe-Weare rule-3 maximum for either the $0(-1,2)$ or $0(2,-1)$ resonance, but unfortunately seems to be missing from the specular beam. Equation (5) predicts minima for the (0,0) and $(-1,1)$ beams and maxima for the others scanned for a $0(-1,2)$ resonance. It predicts all minima except for maxima in the $(-2,-1)$ and $(-1,-1)$ beams for a $0(2,-1)$ resonance. The data do not permit a clear choice between these two alternatives. The disagreement between the two predictions for the specular-beam line shape may be due to the low background in this region of $\vec{K}$ space. In this case, as mentioned above in Sec. II, the prediction of Eq. (5) may fail and a maximum result.

The 0(0,1) resonance near $\theta = 65.5°$ in Fig. 6 shows strong line shapes in all beams, in agreement with both theoretical predictions. This polar angle range should also include a $0(1,-1)$ resonance near $\theta = 63°$, but only very slight indications of it can be seen. The line shape should be a maximum in all

TABLE I. Selective-adsorption line shapes—theory and experiment.

Resonance	Diffraction	Figure	Predictions: Wolfe and Weare[a]	Predictions: Celli *et al.*[b]	Experiment
0(1,0) and 1(1,0)	0,0	3	max,min[c]	min	max,min[d]
	−1,0			min	min
	−2,0			min	min
	0,1			min	min
	−1,1			min	min
	−2,1			min	min
1(1,0) and 2(1,0), degenerate with 1(0,1) and 2(0,1)	0,0	4	min[e]	min[e]	min
	−1,0			min[e]	min
	−2,−1			min[e]	min
	−2,0			min[e]	min
	−1,−1			min[e]	min
	−1,1			max[f],min[g]	max
0(1,1) and 1(1,1)	0,0	5	max	max	max
	−1,0			max	max
	0,1			min	min
	−2,−1			max	max
	−1,1			min	min
	−1,−1			max	max
0(0,1)	0,0	6	min	min	min
	−1,0			min	min
	−2,−1			min	min
	−2,0			min	min
	−1,1			max	max

[a]Reference 8, predictions only for the specular beam.
[b]Reference 7.
[c]That is, a mixed-extrema structure, the maximum dominant.
[d]Variable (see text).
[e]For either a (1,0) or (0,1) resonance; however, note that neither theory is strictly applicable to degenerate cases.
[f]For a (0,1) resonance.
[g]For a (1,0) resonance.

the beams scanned except for a minimum in the $(-2,-1)$ beam. With the exception of the $(-1,1)$ beam, all scans do show a small feature near 63° or 63.5°, in agreement with this prediction.

In summary of the data in Figs. 3 through 6, it can be said that both theoretical predictions are confirmed, with the exception of Eq. (5) applied to a Wolfe-Weare rule-2 resonance. Also, while not strictly applicable to degenerate resonances, both predictions were reasonably accurate when applied to those cases.

The data in Figs. 7 and 8 clearly show the sensitivity of the specular 0(1,0) feature near $\theta = 51°$. According to Wolfe and Weare's work with the optical potential, this rule-2 feature should be especially sensitive to inelastic effects. A change of sample temperature from room temperature to 163 K in Fig. 7 is seen to change the dominant line shape from a minimum to a maximum. The transformation proceeds as a gradual growth of the maximum near $\theta = 50.5°$, while the minimum near 51.5° remains relatively constant with temperature. Thus the mixed extrema structure is readily apparent. As the temperature is lowered there is also an increase in the overall reflected intensity, as expected. The change in sample temperature producing these ef-

fects, about 130 K, does not seem large in relation to the Debye temperature for LiF, 730 K,[26] even if this number is reduced somewhat to reflect surface rather than bulk mean-square displacements. Aside from the overall increase in intensity, most of the other features in the scan do not change. An exception can be seen near $\theta = 44°$ in Fig. 7. There a small maximum can be seen appearing as the temperature is lowered. This is probably the 1(1,0) resonance, also a rule-2 feature, which was not easily separable from the background of other resonances in Fig. 3. These results suggest that rule-2 features are especially sensitive to inelastic effects, confirming the findings of Wolfe and Weare with an optical potential.

The effects of surface temperature on selective-adsorption line shapes were discussed briefly in the work of Krishnaswamy *et al.* for ^{4}He-NaF.[27] In that study the major effort was measurement of the specular-beam Debye-Waller effect with a higher-energy (63 meV) beam. However, with a 17-meV beam it was found that the general features of the scattering pattern were unaffected by a change in surface temperature from 300 to 100 K. Most of the selective adsorption features did not change their character with surface temperature, although more reflected intensity was seen at the lower surface temperature. This is evident in Figs. 3 and 4 of Ref. 27. There is one feature, however, the 0(1,0) near $\theta = 54°$, $\phi = 0°$ (Fig. 3 of Ref. 27), which seems to change from a very shallow minimum at 300 K to a mixed-extrema structure at 100 K. This feature is a rule-2 selective adsorption,[28] suggesting that a similar sensitivity of rule-2 features to inelastic effects may occur in the system ^{4}He-NaF.

Figure 8 shows the sensitivity of the same rule-2 feature to surface aging. The effect of aging is seen to be somewhat akin to that of raising surface temperature. Overall reflected intensity decreases with increasing surface age, but the rule-2 feature shows the most pronounced change. From a very sharp maximum overwhelming its associated minimum just after cleaving, it degrades within a week to a weak maximum dominated by the minimum. As with the sample temperature effect, other features do not show as dramatic a change. Probably the effect of surface aging is to contaminate the surface with adsorbates to some degree. These represent deviations from the perfect periodicity of a clean crystalline surface. The selectively-adsorbed atom moving parallel to the surface in the potential well ought to be susceptible to scattering from the adsorbed molecules, just as it is to interactions with phonons. Either of these will remove it from the elastic scattering process. Thus one might expect to find similar deviations from the clean-surface elastic scattering theory for these two cases. In this context, it should be noted that our earlier work,[17] obtaining excellent agreement with the Wolfe-Weare rule was done with an LiF surface a few hours old held at 130 K. The detailed reasons for the observed special sensitivity of rule-2 features to either effect are not known.

The different detector geometry and surface preparation combinations also affected the quality of results. Figure 9, data taken with detector II and a heated surface, shows the 0(1,0) feature near $\theta = 52°$ as a mixed-extrema line shape, the maximum being of about equal intensity with the minimum. This is in contrast to the results in Figs. 3 or 7 for a freshly-cleaved surface where stronger maxima are seen. A lower overall reflected intensity is also evident. Both of these effects were seen despite the lower sample temperature of 100 K. In comparing these results to the detector-II—cleaved-surface results, it appears that the heated surfaces do not show as much detail or give as much reflection intensity as cleaved ones. Some of these effects, however, may be due to the shorter sample baking time that this sample received relative to those studied with detector I.

The results with detector I on cleaved and heated surfaces suggest that it has a deleterious effect on the elastic scattering process. The detector-I—heated-surface combination yielded a minimum for the rule-2 feature, the only feature whose line shape was inconsistent with the detector-II—cleaved-surface results. This might have been partly due to the detector-I—heated-surface data being taken more than a week after the sample baking had ended. An effect similar to the aging of the cleaved surface in Fig. 8 presumably operates on heated surfaces as well. However, the failure to obtain any reasonable amount of stable reflected intensity with detector I and a cleaved surface strongly suggests that this detector geometry disturbs the elastic scattering. The most obvious possibility is that the bombarding stream of electrons which reach the sample causes some degree of surface damage. A similar effect was suspected in the work of Krishnaswamy *et al.*[27] with ^{4}He-NaF. This damage would then be annealed during the heating and a more damage-resistant surface obtained. In this context, it should be noted that the heating at 850 K for 50—60 h is above average in temperature and length of bake when compared to the heat treat-

ments used by other authors[29] engaged in atom-scattering studies of LiF. Also suggestive of electron impact-induced damage is the rapid decay of reflection intensity while the detector emission current was increased, described at the end of Sec. III. Thus, while stable scattering results can be obtained with detector I by heat treatment of the surface, it is generally inferior to detector II.

V. SUMMARY

We have found that the prediction of Eq. (5) is valid for a variety of selective adsorption features. An exception is a resonance of the Wolfe-Weare rule-2 type. For such a resonance we have observed the mixed-extrema structure predicted by Wolfe and Weare. We have also monitored the conversion of such a feature from a maximum-dominated line shape to a minimum-dominated one under the influence of either sample temperature or contamination. The former is assumed associated with inelastic effects, the latter with a breakdown of potential periodicity. Both affect the rule-2 resonance quite drastically, causing changes in its line shape before effects on other resonances are seen. This confirms the results of a phenomenological treatment of inelastic effects by Wolfe and Weare. The connection between the selective adsorption process and inelastic processes has now been investigated several times.[5,6] It will undoubtedly be of further interest when energy analysis of the scattered beams becomes more common, as is certain to occur in the future.

ACKNOWLEDGMENTS

This investigation was aided by helpful discussions with Professor Milton W. Cole and Professor Vittorio Celli. Advice and technical assistance from Professor Thomas T. Thwaites and Dr. Gianfranco Vidali were also beneficial. The work was supported, in part, by the National Science Foundation under Grant No. DMR 77-22961 and aided by a Grant-in-Aid of Research from Sigma Xi, the Scientific Research Society of North America.

[1]I. Estermann and O. Stern, Z. Phys. 61, 95 (1930); I. Estermann, R. Frisch, and O. Stern, *ibid.* 73, 348 (1932); R. Frisch and O. Stern, *ibid.* 84, 430 (1933).

[2]J. E. Lennard-Jones and A. F. Devonshire, Nature (London) 137, 1069 (1936).

[3]See, e.g., G. Derry, D. Wesner, S. V. Krishnaswamy, and D. R. Frankl, Surf. Sci. 74, 245 (1978); W. E. Carlos and M. W. Cole, Phys. Rev. Lett. 43, 697 (1979).

[4]H. Hoinkes, L. Greiner, and H. Wilsch, in *Proceedings of the Seventh International Vacuum Congress and Third International Conference on Solid Surfaces, Vienna,* edited by R. Dobrozemsky, F. Rüdenauer, F. V. Viehböck, and A. Breth (Berger, Vienna, 1977), p. 349; W. E. Carlos and M. W. Cole, Phys. Rev. Lett. 43, 697 (1979); G. Boato, P. Cantini, and R. Tatarek, Surf. Sci. 80, 518 (1979).

[5]D. Wesner, G. Derry, G. Vidali, T. Thwaites, and D. R. Frankl, Surf. Sci. 95, 367 (1980).

[6]P. Cantini, R. Tatarek, and G. P. Felcher, Surf. Sci. 63, 104 (1977); P. Cantini and R. Tatarek, unpublished.

[7]V. Celli, N. Garcia, and J. Hutchison, Surf. Sci. 87, 112 (1979).

[8]K. L. Wolfe and J. H. Weare, Phys. Rev. Lett. 41, 1663 (1978).

[9]K. L. Wolfe and J. H. Weare, Surf. Sci. 94, 581 (1980).

[10]M. P. Liva and D. R. Frankl, Surf. Sci. 59, 643 (1976).

[11]G. Derry, D. Wesner, S. V. Krishnaswamy, and D. R. Frankl, Surf. Sci. 74, 245 (1978).

[12]H. Chow and E. D. Thompson, Surf. Sci. 54, 269 (1976).

[13]H. Chow and E. D. Thompson, Surf. Sci. 59, 225 (1976).

[14]B. Wood, B. F. Mason, and B. R. Williams, J. Chem. Phys. 61, 1435 (1974).

[15]F. O. Goodman, Surf. Sci. 94, 507 (1980).

[16]N. Cabrera, V. Celli, F. O. Goodman, and J. R. Manson, Surf. Sci. 19, 67 (1970).

[17]D. R. Frankl, D. Wesner, S. V. Krishnaswamy, G. Derry, and T. J. O'Gorman, Phys. Rev. Lett. 41, 60 (1978).

[18]H. Chow, Surf. Sci. 62, 487 (1977).

[19]G. Boato, P. Cantini, R. Tatarek, and G. P. Felcher, Surf. Sci. 80, 518 (1979); G. Boato, P. Cantini, C. Guidi, R. Tatarek, and G. P. Felcher, Phys. Rev. B 20, 3957 (1979).

[20]H. Chow, Surf. Sci. 79, 157 (1979); see also, N. Garcia, W. E. Carlos, M. W. Cole, and V. Celli, Phys. Rev. B 21, 1636 (1980).

[21]J. S. Hutchison, Phys. Rev. B 22, 5671 (1980).

[22]C. E. Harvie and J. H. Weare, Phys. Rev. Lett. 40, 187 (1978).

[23]G. Derry, D. Wesner, G. Vidali, T. Thwaites, and D. R. Frankl, Surf. Sci. 94, 221 (1980).

[24]G. Derry, D. Wesner, S. V. Krishnaswamy, and D. R. Frankl, Surf. Sci. 74, 245 (1978); G. Derry, D. Wesner, W. Carlos, and D. R. Frankl, *ibid.* 87, 629 (1979).

[25]V. Celli, private communication.

[26]J. T. Lewis, A. Lehoczky, and C. V. Briscoe, Phys. Rev. 161, 877 (1967).

[27]S. V. Krishnaswamy, G. Derry, D. Wesner, T. J. O'Gorman, and D. R. Frankl, Surf. Sci. 77, 493 (1978).

[28]This is true if strong coupling for the ^{4}He-NaF system is assumed to mean a first-order reciprocal-lattice vector separating the diffraction and the resonance, as is the case in ^{4}He-LiF.

[29]Some examples are B. R. Williams, J. Chem. Phys. 55, 3220 (1971), 770 K for "a number of hours;" S. S. Fisher and J. R. Bledsoe, J. Vac. Sci. Technol. 9, 814 (1972), 1000 K for 20 min.; G. Boato, P. Cantini, and L. Mattera, Surf. Sci. 55, 141 (1976), 400–600 K for "several hours;" P. Cantini, R. Tatarek, and G. P. Felcher, Surf. Sci. 63, 104 (1977), 600 K for "several hours;" G. Brusdeylins, R. B. Doak, and J. P. Toennies, Phys. Rev. Lett. 44, 1417 (1980), "more than 800 K for at least 12 h." A detailed SIMS study of the adsorption of water vapor was reported in J. Estel, H. Hoinkes, H. Kaarman, H. Nahr, and H. Wilsch, Surf. Sci. 54, 393 (1976). They found no adsorption of water detectable up to an H_2O partial pressure of 10^{-5} Pa with a sample temperature of 170 K following a bake of 700 K for 18 h.